

# Four Quadrant Phase Mask: Analytical Calculation and Pupil Geometry

James P. Lloyd<sup>a</sup>, Donald T. Gavel<sup>b</sup>, James R. Graham<sup>a</sup>,  
Philip E. Hodge<sup>c</sup>, Anand Sivaramakrishnan<sup>c</sup> and G. Mark Voit<sup>c</sup>

<sup>a</sup>Astronomy Department, University of California, Berkeley CA 94720

<sup>b</sup>Lawrence Livermore National Laboratory, Livermore, CA 94551

<sup>c</sup>Space Telescope Science Institute, Baltimore, MD 21218

## ABSTRACT

Of the many novel coronagraphic and nulling techniques that have been suggested to improve image contrast for exoplanet detection, one of the most promising is the Quadrant Phase Mask suggested by Rouan *et al.*<sup>1</sup> Analysis of this optical system has previously been performed by discrete Fourier transform methods, that result in systematic errors due to the implicit assumptions of the methods and mathematical singularities in the transform of the phase mask. In this paper, we describe an analytical treatment of this optical system that treats these singularities explicitly. We calculate the leakage of a Quadrant Phase Mask Coronagraph with these analytical techniques, and show that a Quadrant Phase Mask rejects all on-axis light for an unaberrated, unobscured circular aperture and is therefore a nearly perfect coronagraph. We demonstrate why the Quadrant Phase Mask coronagraph suffers degraded performance with an obscured aperture, and propose modifications to the pupil geometry to mitigate this problem.

**Keywords:** coronagraphs – instruments: miscellaneous – techniques: coronagraphy

## 1. INTRODUCTION

In a phase mask coronagraph the intensity of the image produced by the telescope is left untouched, but a phase mask is inserted to reverse the sign on the electric field vectors over selected areas of this image plane. By phase shifting half of the light by  $\pi$ , the resulting interference will produce a null in the following pupil image. A phase mask, therefore, redistributes light in the following pupil (Lyot) plane, where a pupil stop (known as a Lyot stop) is located. The geometry of both the pupil and phase mask will dictate the distribution of light in the Lyot plane. Roddier *et al.*,<sup>2</sup> Abe *et al.*<sup>3</sup> and Rouan *et al.*<sup>1</sup> have proposed several distinct phase mask geometries. The most attractive of these is the four quadrant phase mask, for its relative simplicity, potentially very deep null, and minimal requirements for undersizing the Lyot stop.

Prior calculations of the quadrant phase mask have relied on numerical simulation, that can give misleading results due to systematic numerical errors. We have therefore investigated analytical methods to calculate the four quadrant phase mask coronagraph, and particularly focus on the effects of pupil geometry.

## 2. THEORY

Following standard Fourier optics theory, the diffraction limited image field  $I(\xi, \eta)$ , formed by a pupil,  $P(u, v)$  obeys the Fourier relationship:  $I(\xi, \eta) = \mathcal{F}(P)$ , where  $\mathcal{F}$  denotes the Fourier transform operation. Similarly, the Lyot field,  $L(u, v)$  is the Fourier transform of the image field. In a coronagraph, the image field is modified by a mask,  $M(\xi, \eta)$ , so the Lyot field is described by:

$$L = \mathcal{F}(I \times M) = \mathcal{F}(I) \star \mathcal{F}(M) = P \star \mathcal{F}(M)$$

---

Further author information: E-mail: jpl@astro.berkeley.edu, Telephone: 1 510 642 8285

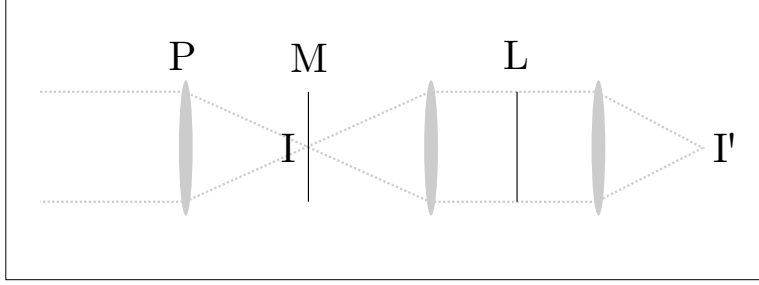


**Figure 1.** The optical layout of a coronagraph consists of three optical elements, to form an image  $I$ , which is filtered by a mask,  $M$ . A re-imaged pupil is then formed at  $L$ , which is again masked before forming the filtered image  $I'$ .

where  $\star$  denotes the convolution operation. The fundamental benefit of a coronagraph is to choose a mask function that results in a favorable distribution of light in the Lyot plane, such that much of the on-axis light can be removed from the final image.

The quadrant phase mask multiplies the image field by

$$M(\xi, \eta) = \frac{1}{2} \text{sgn}(\xi, \eta) = \text{sgn}(\xi) \text{sgn}(\eta)$$

where  $\text{sgn}(x)$  is 1 for  $x > 0$  and  $-1$  for  $x < 0$ . In the Lyot plane this results in a field that is the original aperture function convolved with the transform of  $\frac{1}{2} \text{sgn}(\xi, \eta)$ , *i.e.*,  $-1/(\pi^2 xy)$ .

## 2.1. Square Pupil

The Lyot plane illumination,  $L(x, y)$  can be easily calculated in the case of a square, unobscured aperture of side  $D$ . The convolution is anti-symmetric, we calculate it for the  $x > 0, y > 0$  quadrant here.

$$-\pi^2 L = \ln(F(x)) \ln(F(y)) \quad (1)$$

where  $F$  is a real positive function defined by

$$F(x) = (x + D/2)/(x - D/2) \quad (2)$$

when  $x \geq D/2$ , and

$$F(x) = (D/2 + x)/(D/2 - x) \quad (3)$$

when  $0 \leq x < D/2$ .

Along the coordinate axes  $L$  is zero, since it is antisymmetric. At these points in the pupil plane, the positive and negative parts of the  $1/xy$  function cancel perfectly in the convolution integral. As either  $x$  or  $y$  approach  $\pm D/2$ , (the primary pupil boundary),  $L$  tends logarithmically to  $\pm\infty$  at locations away from the axes. Its sign depends on the quadrant.

As can be seen in Figure 7, the Lyot plane field intensity is very small within most of the pupil for a point source whose image is exactly centered on a perfect quadrant phase mask.

## 2.2. Unobscured Circular Pupil

Prior numerical calculations have performed a numerical Fast Fourier Transform on a phase shifted image. Although this method does not explicitly calculate the  $1/xy$  function, the infinities are still present indirectly, and therefore numerical errors and systematic biases (for example the sampling of the pupil onto a square grid) are still present. Since the low intensity in the pupil plane relies on the perfect (or near perfect) cancellation of a large number of positive and negative infinities in the convolution integral, the correct answer cannot be calculated without extreme care. For the case of an unobscured circular aperture, numerical calculation shows

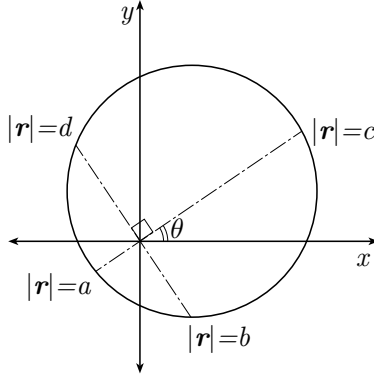


**Figure 2.** Geometry for performing the convolution integral over an offset disk.

that the fraction of light that remains inside the image of the pupil is extremely small. However, our numerical investigation showed that the result was sensitive to the size of the calculation grid, and treatment of subtleties such as the sampling of the pupil boundary and alignment of the mask and image.

Therefore, we have investigated this case analytically. The convolution integral can be written down as:

$$L(u, v) = \frac{-1}{\pi^2} \iint P(x, y) \frac{1}{x-u} \frac{1}{y-v} dx dy \quad (4)$$

Direct methods to calculate this integral, however, fail due to the logarithmic divergence of  $\int 1/x dx$  across  $x = 0$ . Physically, however, the contribution of the  $\pm\infty$  must cancel. This integral can more readily be evaluated by transferring to polar coordinates, centered on the  $1/xy$  function, and integrating over an offset disk.

In polar coordinates, by performing the substitution  $x = r \cos \theta$  and  $y = r \sin \theta$ ,

$$L(u, v) = \frac{-1}{\pi^2} \iint_{\bigcirc} \frac{1}{r \cos \theta} \frac{1}{r \sin \theta} r dr d\theta \quad (5)$$

where the integration is performed over the offset disk as shown in Figure 2, which can be separated into radial and angular integrals:

$$L(u, v) = \frac{-1}{\pi^2} \int \frac{d\theta}{\cos \theta \sin \theta} \int \frac{dr}{r} \quad (6)$$

Breaking the integral over  $dr$  into four rays, one in each quadrant, at a given  $\theta$  between 0 and  $\pi/2$

$$L(u, v) \propto \int_0^a \frac{dr}{r} - \int_0^b \frac{dr}{r} + \int_0^c \frac{dr}{r} - \int_0^d \frac{dr}{r} = \ln \frac{ac}{bd} \quad (7)$$

Considering the geometry of the triangles generated by the chords of the circle, shown in Figure 3, the triangles  $OAD$  and  $OBC$  are similar. Therefore  $a/b = d/c$  or  $ac = bd$  so

$$L(u, v) \propto \ln \frac{ac}{bd} = 0 \quad (8)$$

The intensity in the Lyot plane is zero *everywhere inside the image of P* for an unobscured circular aperture and perfect phase quadrant mask. This result has been independently shown by Rouanet *al.*<sup>4,5</sup>

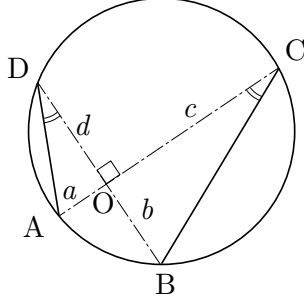


**Figure 3.** Geometry of the triangles generated by the chords of the circle.

### 2.3. Conjugate Pupils

Rouan *et al.*<sup>1</sup> and Riaud *et al.*<sup>6</sup> have noted that the performance of the quadrant phase mask coronagraph degrades markedly with an obscured aperture. Figure 9 shows the intensity in the Lyot plane for an obscured aperture. Light is redistributed around the central obscuration (which remains dark) in the same pattern as outside the pupil. This is because of the result that the Lyot field is identical to within a sign for a conjugated pupil. Consider convolving the following equation with  $1/xy$ :

$$P + (1 - P) = 1 \quad (9)$$

The convolution of  $1/xy$  with 1 is zero, since it is the integral of an odd function in  $x$  and  $y$  over the plane,

$$P \star 1/xy = -(1 - P) \star 1/xy$$

Therefore, since intensity is the square of the field, the intensity produced by a dark aperture embedded in a transmissive one is the same as a transmissive aperture embedded in a dark one. This condition arises due similar symmetries in the equations that gives rise to Babinet's principle, but it is fundamentally different since the diffraction pattern is the re-imaged pupil, and this condition only holds for light on the optical axis.

A small secondary obscuration then behaves like the conjugate of an unobscured circular pupil, as long as the central obscuration is sufficiently small compared to the primary aperture. This line of reasoning also suggests method to mitigate this disadvantage, by modifying the geometry of the central obscuration.

### 2.4. Mitigation of Tip-Tilt Errors by Lyot Undersizing

To achieve the high degree of suppression in the phase quadrant mask, it is necessary that the image be very accurately centered on the crosshair of the mask. If not, the fraction of light phase shifted will no longer be half, resulting in imperfect cancellation. The phase quadrant mask performance is therefore very sensitive to residual tip/tilt errors.<sup>6</sup> In this section we show how to estimate analytically the electric field in the Lyot plane as a result of tip/tilt errors.

To a flat wavefront,  $\phi_0(\vec{a})$ , we add tip-tilt errors,

$$\phi(\vec{a}) = \phi_0(\vec{a}) + \phi_x x + \phi_y y \quad (10)$$

where  $\phi_x = \frac{\partial \phi}{\partial x}$ ,  $\phi_y = \frac{\partial \phi}{\partial y}$  and both are constant.

The Lyot field,  $\mathcal{E}_L(\vec{a})$  is described by:

$$-\pi^2 \mathcal{E}_L(\vec{a}) = \iint_{\odot} \frac{\phi_0(\vec{a}) + \phi_x x + \phi_y y}{xy} dx dy$$

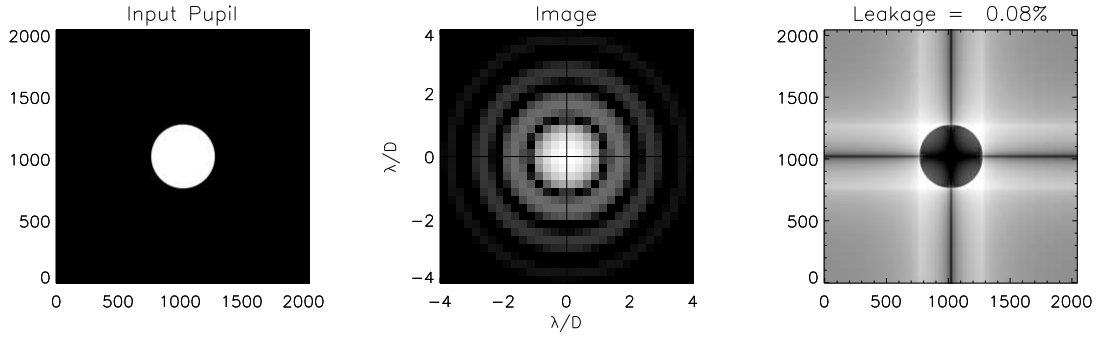


**Figure 4.** Calculation for a sampled-boundary circular pupil (the boundary pixels are fractionally illuminated). The diffraction image of the input pupil is shown for reference, with the center of the quadrant mask marked with the crosshair. As shown in Section 2.2, the interior of the pupil image in the Lyot plane is zero. The 0.08% Leakage figure results entirely from numerical errors arising from both the transform of the mask and the approximation of sampling a circular pupil onto a square grid.

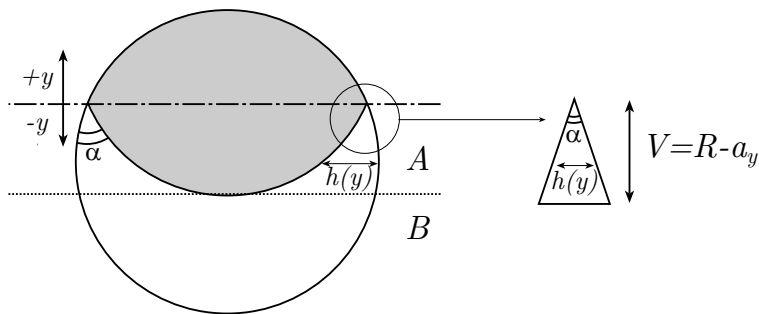


**Figure 5.** Geometry of to evaluate  $\int_{\odot} \frac{dx dy}{y}$ . The shaded region cancels by symmetry. The cusps in region A can be approximated by a triangle for estimation purposes.

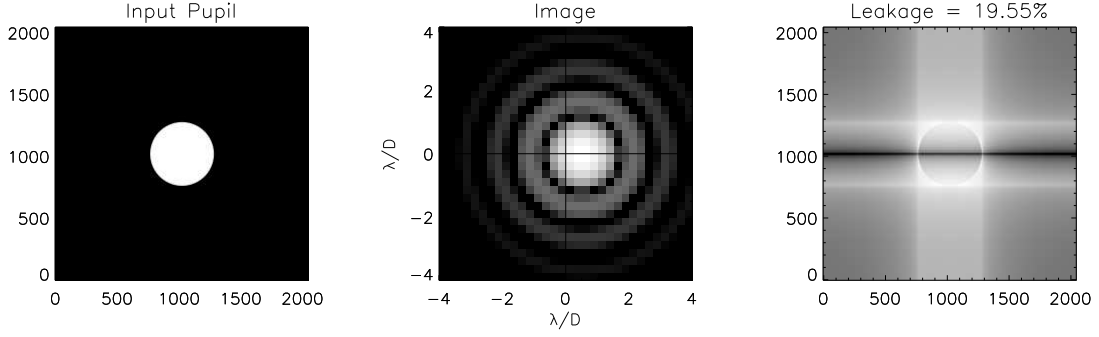


**Figure 6.** The effect of wavefront tilt ( $\lambda/2D$  guiding error) on the Lyot intensity.

or

$$-\pi^2 \mathcal{E}_L(\vec{a}) = \phi_x \int_{\bigcirc} \frac{dx dy}{y} + \phi_y \int_{\bigcirc} \frac{dx dy}{x} \quad (11)$$

We consider only the first term, due to the  $x$ -tilt, the second term is similar. This integral is schematically represented in Figure 5. Once the shaded area is removed from the integration, the area integral can be performed piecewise. The only remaining piece of the singularity in  $1/y$  is at the tip of the triangular cusps in region A, and the integral converges in that region for  $\alpha < \pi$ .

Although the full integral is tractable, it is illuminating to estimate the Lyot field by approximating the integral. In region A, we approximate the triangular cusps with isosceles triangle with the same apex angle. We neglect region B, which will only contribute significantly  $|\vec{a}|$  is close to  $R$ . That is, at the edges of the pupil. Integrating  $1/y$  over the triangular approximations in Figure 5 gives:

$$\int_{\bigcirc} \frac{dx dy}{y} \approx \iint_{\Delta\Delta} \frac{dx dy}{y} = -4 \tan\left(\frac{\alpha}{2}\right) \int_0^V dy = -4(R - a_y) \tan\left(\frac{\alpha}{2}\right)$$

For  $\vec{a} = 0$ ,  $\alpha = 0$ , or at the center of the pupil, the field remains zero.  $\alpha$ , and therefore  $\tan(\frac{\alpha}{2})$  increases in the pupil  $y$  direction. Therefore, an  $x$  tilt introduces light that spills in from the edges of the pupil, in the  $y$  direction, as illustrated in Figure 6.

This observation has the practical advantage that the sensitivity of a four quadrant phase mask coronagraph to residual tip-tilt errors can be reduced by undersizing the Lyot stop.

### 3. PUPIL GEOMETRIES

Modification of the input pupil geometry can drastically change the effect of the phase quadrant mask, one such example being the drastic degradation from perfect cancellation by the introduction of a small obscuration in the center of the mask. In this section we investigate several different illustrative geometries. These calculation are performed using Fast Fourier Transforms on a  $2048 \times 2048$  grid, with a pupil one quarter of the grid in diameter. The boundary of the quadrant mask is aligned with the edge of a pixel (all pixels in  $M$  are -1 or 1) and the image is aligned to the cross-hair of the quadrant mask by applying a phase gradient across the pupil to Fourier-shift the image by half a pixel. The mathematically equivalent approach used by Rouan *et al.*<sup>1</sup> is to center the phase mask on the center of a pixel by introducing a zero value row and column of pixels along the cross-hair, which is equivalent to Fourier-shifting the mask by half a pixel, but results in a mask function that does not conserve flux.

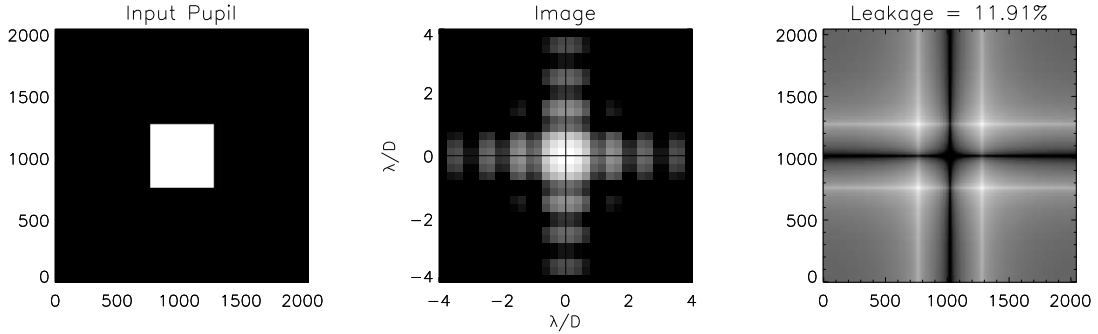


**Figure 7.** Calculation for a square pupil. The left panel shows the input pupil geometry. The center panel is the diffraction image formed by this pupil. The right panel is the distribution of light in the Lyot plane, following the four quadrant phase mask, in logarithmic stretch over 6 orders of magnitude. The “Leakage” figure is the calculated fraction of light that remains in the image of the pupil.

We calculate a simple figure of merit for the four quadrant mask coronagraph which is the fractional transmission of a Lyot stop that is not undersized, or “Leakage”. This is clearly not necessarily optimal in any specific case, but is useful in characterizing the effect of pupil geometry.

It worth noting that since the distribution of light in the Lyot plane is not uniform. The Lyot stop could suppress additional on axis light at the expense of losing some off-axis light, which may be beneficial, as it is in the case of a classical Lyot coronagraph. Additionally, the distribution of light in the final image plane  $I'$  will be modified by the distribution of light in the Lyot plane (ie.  $I'$  is no longer the diffraction PSF of a uniformly illuminated aperture). We do not take account of this in this paper, except to note that the leakage figure of merit is only an approximate indicator of the suppression of the average PSF in the final image.

### 3.1. Square Pupils

The simplest pupils to calculate analytically are square pupils. It is remarkable that the orientation of the pupil with respect to the axes of the quadrant mask dramatically changes the distribution of light in the Lyot plane. The reason for this can be seen by inspecting the convolution integral, Equation 4. If the pupil edges are aligned with the phase mask axes, then the pupil edge is aligned to the singularities in the  $1/xy$  function, and there is a large contribution to the convolution confined to a small area when the pupil edge intersects the singularity, which can be seen as the bright pairs of horizontal and vertical lines in Figure 7. For the rotated pupil (Figure 8), this contribution is distributed more evenly, resulting in a dramatically reduced leakage.

### 3.2. Circular Pupils

As shown in Section 2.2, the perfect, unobscured pupil is completely dark in the Lyot plane inside the image of the pupil. A large fraction (28%) of the light remains within a transcribed square, which results from the contribution of both singularities in the  $1/xy$  function contributing to this region in the convolution. Outside this region, the light intensity falls logarithmically. This light outside the image of the pupil need not be discarded, but can be re-imaged to feed a control loop that accurately keeps the star centered on the mask.

Following the pupil conjugation rule of Section 2.3, a small circular obscuration will replicate the pattern of an unobscured aperture *inside* the pupil, and the interior of the central obscuration remains completely dark.

### 3.3. Modified Obscuration

If an circular aperture is the optimally best shape for a transmissive aperture, then it will be the optimally worst shape for a central obscuration. Therefore, we have investigated several methods to modify the impact central obscuration.

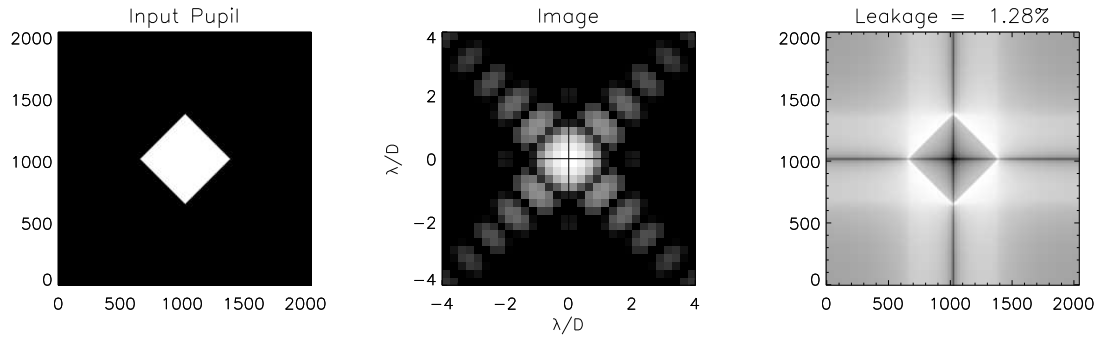


**Figure 8.** Calculation for a rotated square pupil. The realignment of the pupil axes and quadrant mask axes increases the suppression by a full order of magnitude.

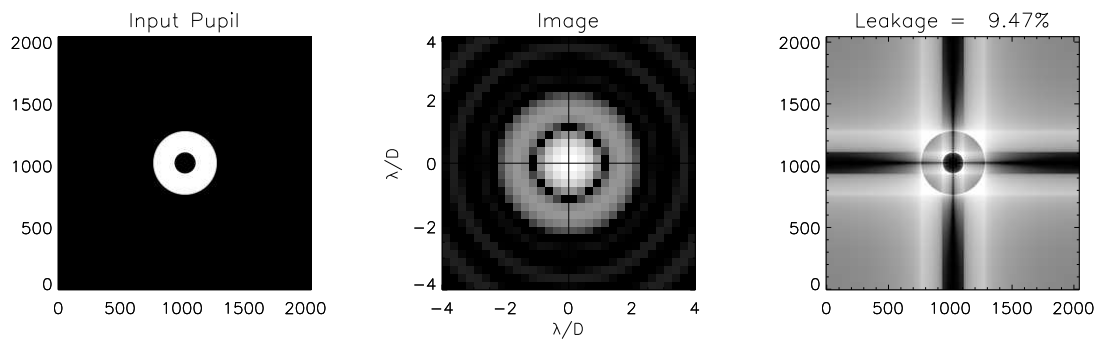


**Figure 9.** Calculation for an obscured (obscuration diameter 0.3 of the primary, typical of wide-field cassegrain telescopes). As shown in Section 2.3, the circular obscuration produces the same pattern as a circular pupil. The 9.5% of the light that passes remains inside the pupil image corresponds very closely to the fractional area of the obscuration.

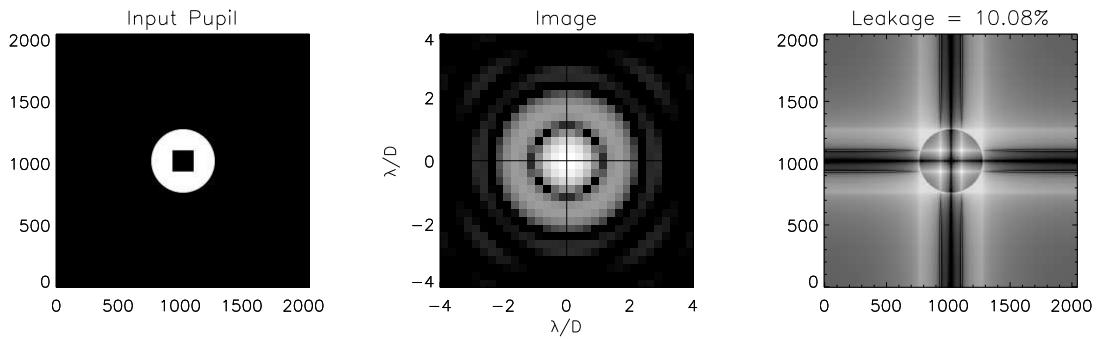


**Figure 10.** Calculation for an obscured pupil with a square obscuration.

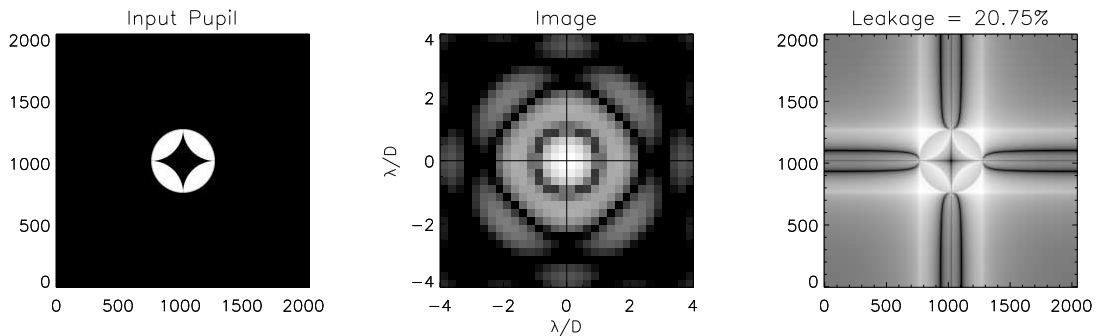


**Figure 11.** Calculation for a “Four Leaf” pupil.

The simplest of these would be to change the shape of the central obscuration. Squaring off the central obscuration results in only a very small loss of light, with the advantage that a much larger fraction of the on-axis light remains inside the central obscuration. The leakage calculated in this specific example is slightly worse than for the circular aperture, however, comparison of Figure 9 and Figure 10 shows that the distribution of light in the Lyot plane is more confined to a much smaller area if the central obscuration is squared off, and an optimal Lyot stop could remove a large fraction of this without excessive penalties to the off-axis transmission. It may therefore be possible to achieve very high suppression even with an obscured telescope if the obscuration can be made small enough.

### 3.4. Concave Pupils

Investigation of the convolution integral shows that the effect of the quadrant mask is to always throw light *outwards* from a concave boundary inside the pupil. We have therefore investigated pupil geometry modifications that attempt to maximize the concave boundary of the pupil constrained to having a central obscuration. We show two cases here, a “Four Leaf” pupil, and a “Four Circle” pupil. As in the case of a square pupil, the orientation of the pupil with respect to the pupil is important. Figures 11–14 show the Lyot plane intensities for these geometries.

The correctly oriented Four Circle pupil retains a great deal of the suppression of a single circular pupil. The calculation here is significantly biased by the numerical errors, and the 0.3% leakage should be regarded as an upper limit. This pupil geometry is amenable to analytical calculation with the methods of Section 2 for an exact result. This geometry is likely to be the most successful for segmented telescopes such as NGST.

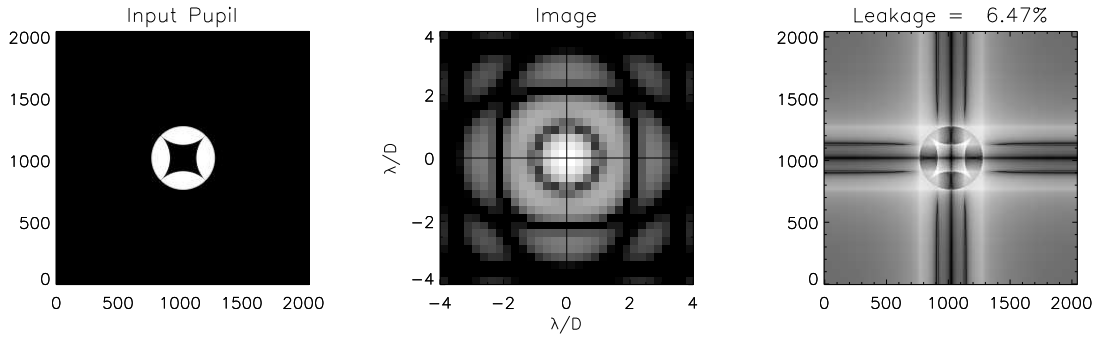


**Figure 12.** Calculation for a rotated “Four Leaf” pupil.

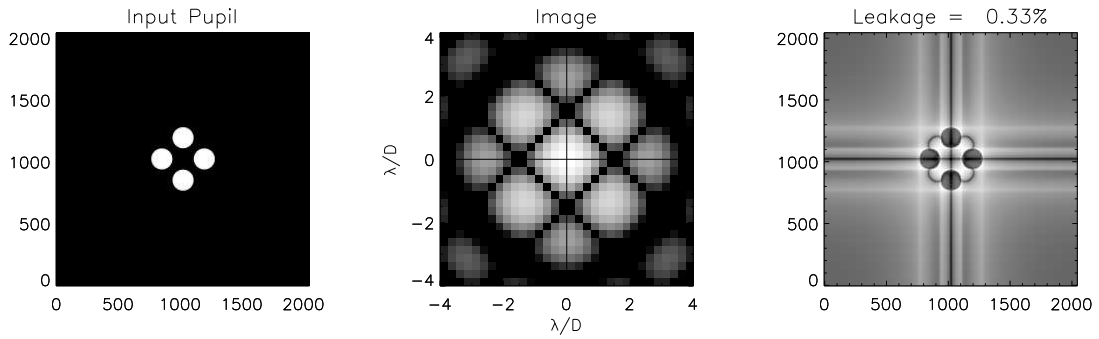


**Figure 13.** Calculation for a “Four Circle” pupil.

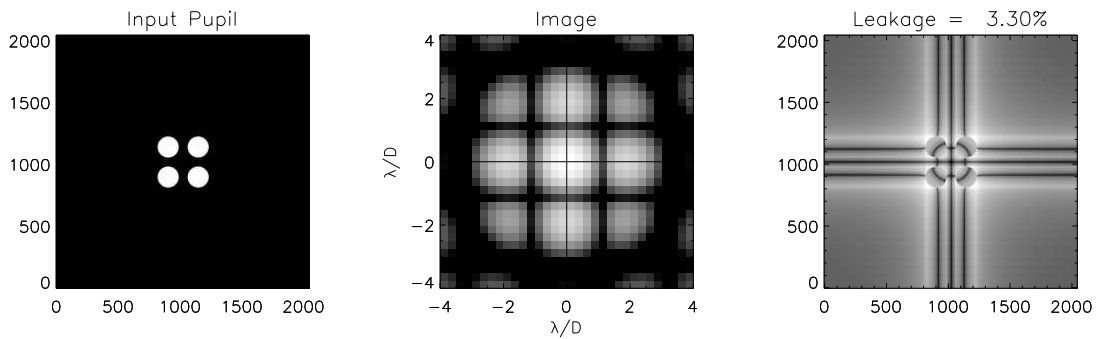


**Figure 14.** Calculation for a rotated “Four Circle” pupil.

## 4. CONCLUSION

We show that the on-axis leakage of a quadrant phase mask coronagraph with a perfect, unobscured circular aperture is zero with analytical methods. This result cannot be reproduced with numerical calculations, even on extremely large grids, due to the effects of aliasing, and the imperfection of sampling a circular pupil onto a square grid. Great care must therefore be taken in interpreting the results of such numerical calculations, which are likely to greatly underestimate the performance of a quadrant phase mask coronagraph in space or with very high order adaptive optics. We also show how to calculate analytically the leakage of a phase quadrant mask due to tip/tilt errors and that this effect can be mitigated by undersizing the Lyot stop.

We have investigated modifications to the input pupil geometry that can mitigate the dramatic performance degradation introduced by a central obscuration in the telescope pupil. For a large central obscuration, masking the pupil into 4 quasi-independent sub-pupils, each circular, is highly effective at restoring the high suppression of the phase quadrant mask. If the central obscuration can be made small enough, modifying its shape to redistribute the light in the Lyot plane can also restore high levels of suppression with an optimized Lyot stop.

## ACKNOWLEDGMENTS

J.L. acknowledges the co-sponsorship of the Australian-American Educational Foundation (Fulbright Commission) and assistance from the Institute of International Education, and the SPIE/Irving J. Spiro Scholarship. This work has been supported in part or full by the National Science Foundation Science and Technology Center for Adaptive Optics, managed by the University of California at Santa Cruz under cooperative agreement No. WAST-9876783. A.S acknowledges funding from the Space Telescope Directors Discretionary Fund.

## REFERENCES

1. D. Rouan, P. Riaud, A. Boccaletti, Y. Cl en et, and A. Labeyrie, “The Four-Quadrant Phase-Mask Coronagraph. I. Principle,” *PASP* **112**, pp. 1479–1486, Nov. 2000.
2. F. Roddier and C. Roddier, “Stellar Coronagraph with Phase Mask,” *PASP* **109**, pp. 815–820, July 1997.
3. L. Abe, F. Vakili, and A. Boccaletti, “The achromatic phase knife coronagraph,” *A&A* **374**, pp. 1161–1168, Aug. 2001.
4. D. Rouan, P. Riaud, and J. Baudrand, “Four quadrants phase mask coronagraphy on large telescopes,” in *Beyond Conventional Adaptive Optics*, R. Ragazzoni, N. Hubin, and S. Esposito, eds. in press.
5. A. Boccaletti, P. Riaud, and D. Rouan, “Speckle Symmetry with High-Contrast Coronagraphs,” *PASP* **114**, pp. 132–136, Feb. 2002.
6. P. Riaud, A. Boccaletti, D. Rouan, F. Lemarquis, and A. Labeyrie, “The Four-Quadrant Phase-Mask Coronagraph. II. Simulations,” *PASP* **113**, pp. 1145–1154, Sept. 2001.